Controlled light-pulse propagation in driven color centers in diamond

Jin-Hui Wu,[1] G. C. La Rocca,[2] and M. Artoni[3,4]
[1]*College of Physics, Jilin University, Changchun 130023, People's Republic of China*
[2]*Scuola Normale Superiore and CNISM, Pisa 56127, Italy*
[3]*Department of Physics and Chemistry of Materials, Brescia University, Brescia 25133, Italy*
[4]*European Laboratory for Nonlinear Spectroscopy, Firenze 50019, Italy*
(Received 25 November 2007; published 26 March 2008)

Inhomogeneously broadened optical transitions of nitrogen-vacancy centers in diamond may be employed to attain fully developed photonic band-gap structures with negligible absorption via coherent optical nonlinearities. For realistic material parameters, the resulting band gap may be tuned via the coupling field to acquire reflectivities very close to unity and sufficiently large bandwidths. We anticipate that this can be used to optically control with remarkable experimental simplicity the reflected and transmitted parts of an incident light pulse.

DOI: 10.1103/PhysRevB.77.113106 PACS number(s): 42.70.Qs, 42.50.Gy

An ever increasing effort has been devoted over the years to develop techniques for manipulating light in optical devices. Electromagnetically induced transparency (EIT)[1,2] is one among the most attractive techniques that has recently led to an astonishing control on light wave propagation. Submillimeter sized cigar-shaped clouds of alkali atoms driven by a "traveling" light wave and cooled to within a millionth of a degree above absolute zero are just paradigmatic examples. In such samples, group velocities[3] as low as 1 m/s and light-pulse storage and retrieval,[4] e.g., have been attained. Yet, when the same three-level atom is driven by a "standing" light wave,[5] the probe optical response is modulated periodically in space. This realizes a photonic band-gap structure[6] where the underlying medium is homogeneous, the band structure being, in fact, fully controlled through the external standing light wave form. Such a scheme has been used, e.g, to reversibly convert a light pulse into a stationary excitation inside a dilute volume of atoms.[7]

For many potential applications, however, solid-state solutions are preferred owing to obvious advantages, such as high atomic densities, absence of atomic diffusion, compactness, simplicity, and scalability, just to mention a few. Early work on control over photonic band gap comprises, e.g., structures built from the periodic complex susceptibility of quantum well excitons whose optical properties can be dynamically modified through the Stark effect.[8] Other interesting proposals to control photonic band gaps in semiconductor heterostructures have been brought forward,[9] and where control over the band gap is achieved through EIT in conduction intersubband transitions of a n-doped quantum well. EIT effects have actually been observed not only in semiconductor quantum wells[10] but also in a class of solid materials exhibiting defect states, following either familiar[1,2] or less familiar[11–13] schemes, and among which[14,15] presodimium-doped Y_2SiO_5 and diamond containing nitrogen vacancy (N-V) color centers[16,17] are perhaps the most ubiquitous ones.

Color centers in diamond, in particular, have attracted over the past few years a renewed interest for their potential as single-photon sources[18] and as quantum memories[19] in solids. These N-V color centers are attractive qubit candidates as they behave a bit like an atom trapped in the diamond lattice. Composed of a substitutional nitrogen next to a carbon vacancy, these centers can have extremely long-lived spin coherence because the diamond lattice is composed primarily of ^{12}C, which has zero nuclear spin. In addition to its promising prospect as a qubit candidate, N-V color centers also have interesting optical properties as they exhibit a configuration with two ground state levels connected to a common excited state by optical transitions of moderate strength, leading to a lambda-type level configuration required for the observation of EIT.[17] This has, in turn, been exploited to devise an all-optically tunable photonic band-gap mechanism whose basic features have recently been addressed by considering a rather simplified analytical model.[20]

In this Brief Report, we extend this previous work to include for a realistic Gaussian profile of the levels' inhomogeneous broadening and by referring to a realistic energy level distribution as it occurs, e.g., in strained diamond N-V centers.[21] We first numerically evaluate the photonic band-gap profiles for this specific N-V diamond crystal configuration. We then study the propagation of an optical pulse in the band-gap region. Transmission and reflection for incident probe pulses are here obtained by using a direct Fourier-transform method. Our calculations show reflectivities exceeding 99% in a millimeter long diamond sample when most probe frequency components lie inside the band gap, yielding instead controllable loss and distortion as the incident probe pulse falls outside the gap.

We start by considering a single three-level impurity dressed by a coupling field ω_c and a probe field ω_p. The three levels $|a\rangle$, $|b\rangle$, and $|c\rangle$ are shown in Fig. 1. In the limit of a weak probe, the steady state off-diagonal density matrix element ρ_{ab} is

$$\rho_{ab} = \frac{i\Omega_p\{[\Gamma_{cb}|X|^2 + \gamma_{ab}\Omega_c^2]Y - \Gamma_{cb}\Omega_c^2 X\}}{Z[2\Gamma_{cb}|X|^2 + \gamma_{ab}(1 + 3\Gamma_{cb}/\Gamma_{ab})\Omega_c^2]},$$

$$X = \gamma_{ab} + i(\Delta\omega_{ab} - \Delta\omega_{cb}),$$

$$Y = \gamma_{cb} + i(\Delta_p + \Delta\omega_{cb}),$$

$$Z = [\gamma_{ab} + i(\Delta_p + \Delta\omega_{ab})]Y + \Omega_c^2. \quad (1)$$

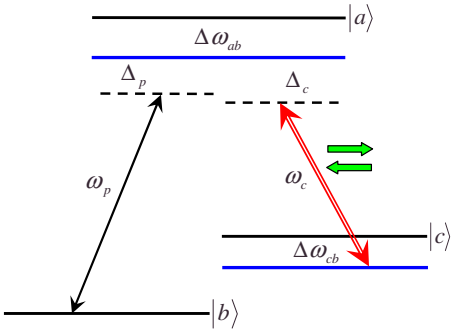

FIG. 1. (Color online) Schematic three energy-level configuration for N-V color center in a diamond sample. The blue (dark gray) lines denote the inhomogeneous line centers of levels $|a\rangle$ and $|c\rangle$ for all active sites in the sample. For negatively charged N-V centers (Ref. 21), the two lower levels belong to the ^3A spin triplet manifold with a 2.88 GHz splitting between the $m_s=0$ ($|b\rangle$) and the $m_s=\pm 1$ ($|c\rangle$) states. They are connected to level $|a\rangle$, belonging to the strain-split ^3E manifold, by optical transitions of moderate strengths.

Here, Γ_{ab}, Γ_{ac}, Γ_{cb}, and Γ_{bc} are the population decay rates, while γ_{ab}, γ_{ac}, and γ_{cb} denote the coherence decay rates. $\Delta\omega_{cb}$ and $\Delta\omega_{ab}$, sensitive to the impurity local environment, represent deviations of the resonant frequencies of the three-level system from the centers of the inhomogeneous lines, contributed by all active impurities. Here, Δ_p is the detuning of the probe field from the $|b\rangle-|a\rangle$ inhomogeneous line center, while Ω_c and Ω_p are the coupling and probe field Rabi frequencies, respectively. In deriving Eq. (1), we have assumed a coupling field resonant with the $|c\rangle-|a\rangle$ inhomogeneous line center, i.e., $\Delta_c\equiv 0$. Moreover, $\Gamma_{cb}=\Gamma_{bc}$, $\gamma_{ab}=\gamma_{ac}$, and $\Delta\omega_{ac}=\Delta\omega_{ab}-\Delta\omega_{cb}$ have been taken into account. We consider the case where the coupling field has a standing-wave pattern as that generated from the retroreflection upon a mirror of reflectivity R_m. The resulting squared coupling Rabi frequency varies periodically in x as

$$\Omega_c^2=\Omega_0^2[(1+\sqrt{R_m})^2\cos^2(k_cx)+(1-\sqrt{R_m})^2\sin^2(k_cx)], \quad (2)$$

with a spatial periodicity a which is half the coupling field wavelength in the medium $\lambda_c=2\pi/k_c=2\pi c/\omega_c n_b$, where $n_b=2.4$ is the background index of refraction of diamond.[22] The forward (FD) and backward (BD) coupling fields may be misaligned through an angle θ, which changes the periodicity as $a=\lambda_c/[2\cos(\theta/2)]$.

The probe linear susceptibility contributed by all active impurities can be easily obtained by integrating over the inhomogeneous broadening distribution of detunings $\Delta\omega_{cb}$ and $\Delta\omega_{ab}$ the quantity $\mathcal{N}|d_{ab}|^2\rho_{ab}/2\varepsilon_0\hbar\Omega_p$, where $\mathcal{N}$ is the impurity density and d_{ab} the electric dipole transition matrix element. For a Gaussian broadening profile, we are required to evaluate

$$\chi(\Delta_p)=\frac{1}{\pi W_{cb}W_{ab}}\int e^{-\Delta\omega_{cb}^2/W_{cb}^2}d(\Delta\omega_{cb}) \times\int e^{-\Delta\omega_{ab}^2/W_{ab}^2}\frac{\mathcal{N}|d_{ab}|^2}{2\varepsilon_0\hbar}\frac{\rho_{ab}}{\Omega_p}d(\Delta\omega_{ab}), \quad (3)$$

with W_{cb} (W_{ab}) the inhomogeneous linewidths on transitions $|c\rangle\leftrightarrow|b\rangle$ ($|a\rangle\leftrightarrow|b\rangle$), from which the frequency dependent probe refractive index $n(\Delta_p)=\sqrt{\chi_b+\chi(\Delta_p)}$ can be evaluated ($\chi_b=n_b^2$). Clearly, n also depends on the position and is periodic in the x direction so that a photonic band gap is expected to occur at the Brillouin zone boundary π/a. Using the spatially dependent refractive index, we can further numerically calculate a 2×2 unimodular transfer matrix M,[23] which describes the propagation of a monochromatic probe field through a single period of the dressed medium and characterizes the band-gap structure. In fact, the translational invariance of the periodic medium requires,[24] i.e.,

$$\begin{bmatrix}E^+(x+a)\\E^-(x+a)\end{bmatrix}=M\begin{bmatrix}E^+(x)\\E^-(x)\end{bmatrix}=\begin{bmatrix}e^{i\kappa a}E^+(x)\\e^{i\kappa a}E^-(x)\end{bmatrix}, \quad (4)$$

where E^+ and E^- denote the FD and BD propagating probe electric fields, respectively, and where $\kappa=\kappa'+i\kappa''$ is the probe Bloch wave vector of photonic states. The photonic band-gap structure can be numerically obtained from solutions of the determinantal equation $e^{2i\kappa a}-\mathrm{Tr}(M)e^{i\kappa a}+1=0$, with $\det M=1$.[24] For a sample of finite length $L=Na$, with N being the number of standing-wave periods, the total transfer matrix $M_N=M^N$ can be expressed[24] in terms of the single period transfer matrix M, and the reflection and transmission amplitudes for the probe can be written as

$$r(\Delta_p)=\frac{M_{N(12)}(\Delta_p)}{M_{N(22)}(\Delta_p)}, \quad t(\Delta_p)=\frac{1}{M_{N(22)}(\Delta_p)}, \quad (5)$$

from which the reflectivity $R=|r|^2$ and the transmissivity $T=|t|^2$ can be easily calculated.

Starting from Eq. (5), we can study the propagation properties of an incident probe pulse. In fact, as we limit ourselves to low intensity probe pulses, the linear response functions r and t derived above for a monochromatic probe field contain all the relevant information on the response of the coherently driven sample. Decomposing the input pulse in its Fourier components, the transmission or reflection process is calculated using Eq. (7), and then the transmitted and reflected pulses can be reconstructed via the inverse Fourier transform. Here, we assume that the input probe has Gaussian profiles in the time and frequency domains, i.e.,

$$E_{It}(t)=E_{0t}e^{-(t-t_0)^2/\Delta t^2},$$

$$E_{If}(\Delta_p)=E_{0f}e^{-(\Delta_p-\Delta_{p0})^2/\delta_p^2}, \quad (6)$$

where t_0 and Δt (Δ_{p0} and δ_p) are the center and the half-width of the incident probe pulse in the time (frequency) domain, respectively. Note that $\delta_p=2/\Delta t$ and $E_{0f}=\sqrt{\pi}\Delta t E_{0t}$. Then, the reflected and transmitted electric field pulse profiles for each frequency component are obtained from $E_{\mathrm{Rf}}(\Delta_p)=E_{If}(\Delta_p)\cdot r(\Delta_p)$ and $E_{Tf}(\Delta_p)=E_{If}(\Delta_p)\cdot t(\Delta_p)$, so that

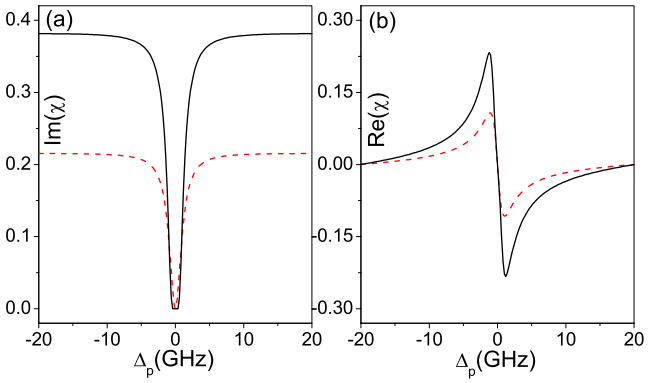

FIG. 2. (Color online) Imaginary and real parts of the susceptibility [Eq. (3)] for N-V diamond driven by a traveling wave (R_m=0.0) with Ω_{c0}=20.0 GHz. Solid and red dashed curves refer respectively to inhomogeneous Gaussian and Lorentzian broadening profiles.

$$E_{Rt} = \int E_{\mathrm{Rf}}(\Delta_p) e^{i(\Delta_p - \Delta_{p0})t} d(\Delta_p),$$

$$E_{Tt} = \int E_{Tf}(\Delta_p) e^{i(\Delta_p - \Delta_{p0})t} d(\Delta_p) \quad (7)$$

yield the reflected and transmitted probe pulse time dependence in terms of the incident probe shape.

Following this procedure, we now illustrate how pulse propagation in N-V diamond color center samples may be all-optically controlled. We adopt here realistic parameters as taken from recent experiments on coherent population trapping in N-V color centers,[21] in particular, using as inhomogeneous linewidths the values W_{ab}=375 GHz and W_{cb}=2.5 MHz. Probe absorption and dispersion are shown in Fig. 2, where they are further compared with those obtained earlier[20] by using a Lorentzian inhomogeneous broadening profile. Owing to the long tails of a Lorentzian broadening distribution, the corresponding EIT window turns out to be shallower than the one obtained by using a Gaussian inhomogeneous broadening profile. In the latter case, the reduced values of residual absorption in the EIT region are, in turn, responsible for the well developed photonic band-gap structure reported in Fig. 3. Correspondingly, probes with frequencies inside the band gap will experience almost perfect reflection (over 99%) for a sample of finite length as shown in Fig. 4(a). Reflection and transmission in Figs. 4(a) and 4(b) display, in addition, rapid oscillations (fringes) near the band gap due to the interference arising from the front and back surfaces of the sample. The presence of fringes, however, is tightly related to the background absorption Im(χ_b). When this is properly included[25] in the expression for the refractive index used to evaluate the spectra in Figs. 4(a) and 4(b) (dotted curves), it can, in fact, well smooth out the oscillations yet maintaining high values of the reflectivity.

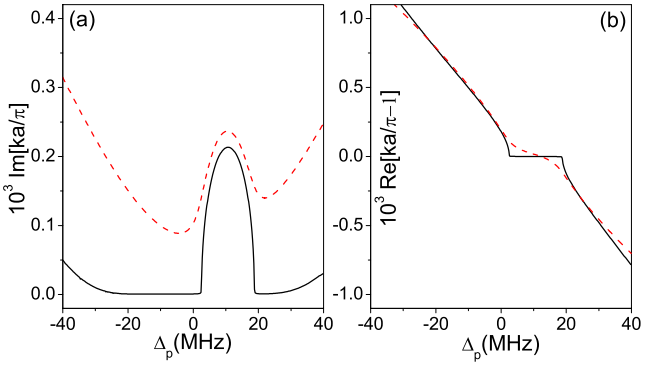

FIG. 3. (Color online) N-V diamond photonic band gap near the first Brillouin zone boundary induced by a standing-wave coupling field with Ω_{c0}=20.0 GHz, R_m=0.617, and θ=38.0 mrad. The notation is the same as in Fig. 2.

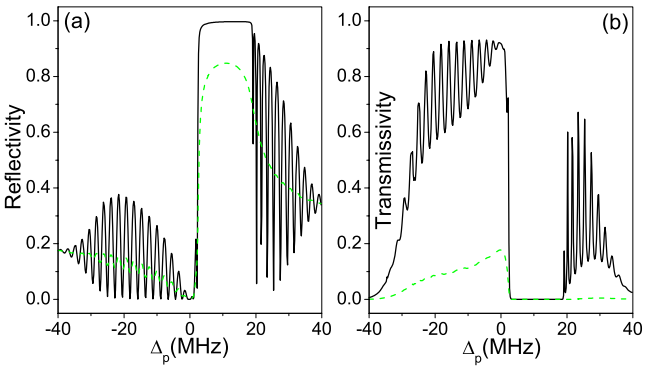

FIG. 4. (Color online) Probe reflectivity and transmissivity spectra for a 2.0 mm long N-V diamond sample. The green dashed curves correspond to a background absorption of Im(χ_b)=0.0002. The standing-wave driving field parameters are the same as in Fig. 3.

In Fig. 5, we show the reflected and transmitted probe

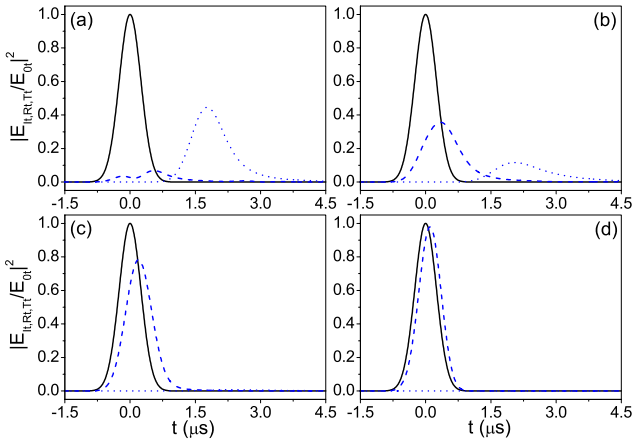

FIG. 5. (Color online) Pulse dynamics of an incident (black solid) probe impinging upon a 2.0 mm long N-V diamond sample. The parameters of the standing-wave coupling field again are the same as in Fig. 3, while the reflected (blue dashed) and transmitted (blue dotted) intensities are scaled to the incident probe pulse peak intensity. Frequency widths and centers of the incident probe pulses are δ_p=4.0 MHz and (a) Δ_{p0}=0.0, (b) Δ_{p0}=3.0 MHz, (c) Δ_{p0}=6.0 MHz, and (d) Δ_{p0}=10.0 MHz.

pulse intensities. When all frequency components of the probe are inside the band gap [see Fig. 5(d)], the reflected pulse has essentially no loss or deformation. Conversely, the reflected pulse is increasingly suppressed and distorted as the probe frequency carrier gradually moves away from the center of the stop band. Simultaneously, a stronger transmitted pulse is observed.

In summary, the propagation dynamics of a probe pulse in N-V diamond color center samples can be suitably tailored through an all-optically induced photonic band gap whose properties have been thoroughly investigated here. Our numerical simulations show that a well developed photonic band gap opens up in the EIT window as a result of the periodically modulated refractive index of the coherently driven N-V diamond material. Band-gap reflectivities over 99% for a 2.0 mm long diamond sample of N-V can be attained for realistic material parameters. Such a controllable stop-band mechanism may easily be exploited to devise a dynamically tunable "beam splitter" for single-photon probe pulses for quantum communication processing purposes.

We would like to thank M. Santoro for enlightening discussions. We greatly acknowledge financial support from the NSFC (No. 10404009), the 973 program (2006CB921103), the NCET, the JDYS (No. 20070121), the MIUR-PRIN (No. 2006-021037), and the Actione Integrada (IT-1603). J.-H. W. is grateful for the hospitality at Scuola Normale Superiore in Pisa.

[1] S. E. Harris, Phys. Today **50**(7), 36 (1997).
[2] M. Fleischhauer, A. Imamoglu, and J. P. Marangos, Rev. Mod. Phys. **77**, 633 (2005).
[3] L. V. Hau, S. E. Harris, Z. Dutton, and C. H. Behroozi, Nature (London) **397**, 594 (1999).
[4] C. Liu, Z. Dutton, C. H. Behroozi, and L. V. Hau, Nature (London) **409**, 490 (2001).
[5] R. Corbalán, A. N. Pisarchik, V. N. Chizhevsky, and R. Vilaseca, Opt. Commun. **133**, 225 (1997); H. Y. Ling, Y. Q. Li, and M. Xiao, Phys. Rev. A **57**, 1338 (1998); M. Mitsunaga and N. Imoto, *ibid.* **59**, 4773 (1999).
[6] K. Sakoda, *Optical Properties of Photonic Crystals* (Springer, Berlin, 2001).
[7] M. Bajcsy, A. S. Zibrov, and M. D. Lukin, Nature (London) **426**, 638 (2003).
[8] J. Prineas, J. Zhu, and J. Khul, Appl. Phys. Lett. **81**, 4332 (2002).
[9] S. M. Sadeghi, W. Li, and H. M. van Driel, Phys. Rev. B **69**, 073304 (2004); S. M. Sadeghi and W. Li, *ibid.* **72**, 165341 (2005); S. M. Sadeghi, W. Li, X. Li, and W. P. Huang, *ibid.* **73**, 035304 (2006).
[10] M. C. Phillips, H. Wang, I. Rumyantsev, N. H. Kwong, R. Takayama, and R. Binder, Phys. Rev. Lett. **91**, 183602 (2003).
[11] E. Baldit, K. Bencheikh, P. Monnier, J. A. Levenson, and V. Rouget, Phys. Rev. Lett. **95**, 143601 (2005).
[12] M. Bigelow, N. N. Lepeshkin, and R. W. Boyd, Science **301**, 200 (2003).
[13] F. Jelezko, T. Gaebel, I. Popa, A. Gruber, and J. Wrachtrup, Phys. Rev. Lett. **92**, 076401 (2004).
[14] B. S. Ham, M. S. Shahriar, and P. Hemmer, Opt. Lett. **22**, 1138 (1997); B. S. Ham, P. Hemmer, and M. S. Shahriar, Opt. Commun. **144**, 227 (1997).
[15] A. V. Turukhin, V. S. Sudarshanam, M. S. Shahriar, J. A. Musser, B. S. Ham, and P. R. Hemmer, Phys. Rev. Lett. **88**, 023602 (2001).
[16] C. Wei and N. B. Manson, Phys. Rev. A **60**, 2540 (1999).
[17] P. Hemmer, A. V. Turukhin, M. S. Shahriar, and J. A. Musser, Opt. Lett. **26**, 361 (2001).
[18] C. Kurtsiefer, S. Mayer, P. Zarda, and H. Weinfurter, Phys. Rev. Lett. **85**, 290 (2000).
[19] L. Childress, J. M. Taylor, A. S. Sorensen, and M. D. Lukin, Phys. Rev. Lett. **96**, 070504 (2006).
[20] Q.-Y. He, Y. Xue, M. Artoni, G. C. La Rocca, J.-H. Xu, and J.-Y. Gao, Phys. Rev. B **73**, 195124 (2006); Q.-Y. He, J.-H. Wu, T.-J. Wang, and J.-Y. Gao, Phys. Rev. A **73**, 053813 (2006); see also E. Kuznetsova, O. Kocharovskaya, P. Hemmer, and M. O. Scully, *ibid.* **66**, 063802 (2002), where the same Lorentzian inhomogeneous broadening distribution has been used for analytical convenience.
[21] C. Santori, D. Fattal, S. M. Spillane, M. Fiorentino, R. G. Beausoleil, A. D. Greentree, P. Olivero, M. Draganski, J. R. Rabeau, P. Reichart, B. C. Gibson, S. Rubanov, D. N. Jamieson, and S. Prawer, Opt. Express **14**, 7986 (2006).
[22] The driving field strength [see Eq. (2)] slightly differs from the one used in Ref. 20, where a simplified analytical model which did not account for the background index of refraction has been adopted and, hence, lead to different values of periodicity a. The background refractive index also causes spurious reflections which have been here accounted for by putting antireflection coatings on the sample entrance and exit faces when drawing Figs. 4 and 5.
[23] M. Born and E. Wolf, *Principles of Optics*, 7th (expanded) ed. (Cambridge University Press, Cambridge, England, 1999).
[24] M. Artoni and G. C. La Rocca, Phys. Rev. Lett. **96**, 073905 (2006); M. Artoni, G. C. La Rocca, and F. Bassani, Phys. Rev. E **72**, 046604 (2005).
[25] A susceptibility $\mathrm{Im}(\chi_b)=0.0002$ corresponds to a background absorption coefficient $\alpha_b \approx 4\ \mathrm{cm}^{-1}$, which is here purposely overestimated to show the effect of background absorption on fringes. Depending, in fact, on the sample preparation and temperature, much smaller values of α_b, are in order (Ref. 26), making, in turn, the effect of absorption on the band-gap reflectivity unimportant in actual samples.
[26] G. Davies and M. Hamer, Proc. R. Soc. London, Ser. A **348**, 285 (1976); see also A. Collins, *The Physics of Diamond*, Proceedings of the Varenna School Course CXXXV (IOS, Amsterdam, 1997), p. 273.